Tellus (1985), *37A*, 323–335

500 mb geopotential height spectral peaks in the 1- to 5-week range

By JUHANI RINNE and ANNAKAISA SARKANEN, *Department of Meteorology, University of Helsinki, Hallituskatu 11–13, SF-00100 Helsinki 10, Finland*

(Manuscript received February 9, 1984; in final form March 5, 1985)

ABSTRACT

Spectral peaks in the range of 1 to 5 weeks are computed from the empirical orthogonal functions of the 500 mb geopotential height, 1946–79. The maximum entropy method is employed. The problems of the method are discussed. A number of peaks are found. Tentative explanations in terms of various Rossby modes may be offered as follows: 16, 5 and 4.5–4 day peaks as symmetric modes, 9 and 7 day peaks as antisymmetric modes and the 2.5 day peak as a Rossby-gravity mode. No explanation for 3, 6, 12 and approximately 30-day peaks are proposed. The 30-day peak is often the most dominant peak in the spectra in which it occurs.

1. Introduction

Deland (1965) and Eliassen and Machenhauer (1969) computed the phase velocities of Rossby modes. They studied the amplitudes of the spherical harmonics computed from analyses of the 500 mb geopotential height. The latter authors found quite a good agreement with their theoretical computations (cf. Dikii and Golitsyn, 1968). Observations of travelling Rossby waves up to the 1980's have been comprehensively reviewed in Madden (1979). The recent theoretical results take into account the variation of the mean field. Kasahara (1980) varied the basic zonal flow. Salby (1981a, b) included realistic vertical and meridional mean wind variations when estimating the uncertainty of eigenfrequencies. He concluded that "several initial modes for the first few wavenumbers should be both realizable and identifiable in typical conditions". Further, "the response of the Rossby modes will necessarily be suppressed and diffused beyond identification for sufficiently large zonal and meridional wavenumbers".

Prior to the 1970's, "practically every period from 3 to 40 days has been reported", as can be concluded from Table 4 in Madden (1979). During the 1970's, the 5-day (e.g. Madden and Julian, 1972) and 16-day (e.g. Madden, 1978) waves were found in the troposphere in many connections. Otherwise spectral studies tended to discuss only the general features of the spectra. In his detailed study of 500 mb spectra, Willson (1975) mentions no peak periods. Blackmon (1976) describes only the periods of 5 and 15 days in the extratropical areas. Schäfer (1979) finds the largest amplitudes of the zonal waves $m = 1$ and $m = 2$ at periods of 5 and 18 days. At lower latitudes, the westward moving 5-day wave with the zonal wavenumber $m = 2$ is split into two parts having periods near 10 and 4 days. In addition, Fräedrich and Böttger (1978) found spectral peaks at 20–30 days in the stationary ultralong waves and at 10 and 4–6 days in the eastward propagating long waves. McGuirk and Reiter (1976) and Webster and Keller (Southern Hemisphere) (1975) have identified a vacillation at about 24 days in hemispheric-scale energy parameters. Other tropospheric periods in the range of a few weeks are rarely discussed in recent literature.

Up to now, the strongest observational evidence in the troposphere has been mainly related to 16- and 5-day waves. These correspond to the symmetric modes that are identifiable in typical conditions, in terms of Salby (1981b). Both theoretical and observational work is based on the Rossby modes or on the normal modes of the prediction equations. Usually the modes include no climatological information (an exception are the vertical part of modes in Bradley and Wien-Nielsen (1968)). They are derived from models which are linearized with respect to a single basic flow and which have no forcing terms that are important on the climatological time scale. In contrast to that, the empirical orthogonal functions (EOF) are derived from observations. Particularly the low-indexed EOFs explain most of the variance in the longer periods (Rinne and Sarkanen, 1983a). Thus the spectral analysis of EOF components can give another viewpoint for the existence of oscillations on the time scale of a few weeks.

The aim of the present study was to list all of the peaks for the 500 mb geopotential height, as found in the range of 1–5 weeks in the spectra of the EOFs. Because the number of peaks is large, a detailed study of them has to be done in other connections. Similarly, the seasonal variation cannot be taken into account. In the present paper, our main interest is to find the peaks. Their significance is studied only from the point of view of their recurrence. A peak is considered more significant if it is found in many (all) subsamples and in many EOFs.

In the spectral analysis, we will apply the maximum entropy method (MEM). The correct determination of the filter length, or resolution, is difficult. Because we have divided our time series into four subsamples, it is possible to compare the results of filter lengths in different samples and study the significance of the spectral results. Thus, besides the peak lists, we will present some comments on the behaviour of the MEM.

2. The data

The main data consist of 14,672 FNWC (Fleet Numerical Weather Center) analyses of the 500 mb height for the 25-year period 1946–70. The mean field and the EOF functions are computed using 11,876 analyses of the 500 mb geopotential height (Rinne et al., 1981). The data are given in the FNWC grid, a total of 1404 points north of 20° N. The way in which the present functions are determined and the representativeness of the functions are discussed in Rinne and Karhila (1979) and in Rinne and Järvenoja (1979), respectively. The coefficients are also computed for the years 1966–79 using the same functions and NMC (National Meteorological Center) analyses. This independent data consist of 10,017 analyses.

The total variance of the 11,876 analyses mentioned is 25,175 m^2. The leading components up to $N = 1, 10, 100$ and 175 explain 57.7, 79.0, 98.7 and 99.5 % of the total variance, respectively.

The time series of coefficients $C_\nu(t)$ are divided into four parts that partly overlap: 1946–55, 1955–62, 1962–70 and 1966–79. Note, that in all samples we apply the same EOFs, which are initially determined from a very large sample. The FNWC and NMC series do not together form stationary time series. A comparison of the NMC–FNWC analyses for the overlapping period showed some disagreement and so they have been investigated separately. Data values are given twice a day, at 00 and 12 GMT, except during the period 1946–55, when only once a day, at 12 GMT. The missing coefficients are interpolated linearly.

Except for the first component, no prewhitening or detrending were applied. Experiments with high-pass filters suppressing cycles longer than two months were made. The use of such filters did not change the results at shorter periods. In the case of the first component it was necessary to remove the dominant annual and semiannual cycles.

3. The spectral method and computations

According to the maximum entropy method (MEM), the spectral density is found from

$$S(f) = \frac{P_{M+1}}{2f_N \left| 1 + \sum_{j=1}^{M} \gamma_j \exp(-i2\pi f \cdot j\Delta t) \right|^2}. \tag{1}$$

Here M, P_{M+1} and coefficients γ_j have first to be determined, The Nyquist frequency is f_N and Δt is the uniform sampling interval.

The method is essentially based on the use of the prediction error filter (Peacock and Treitel, 1969). The variance of the prediction error is given by P_{M+1}. Parameters γ_j ($j = 1, \ldots, M$) are coefficients of the prediction equation. The parameter M determines the oldest observation ($t - M\Delta t$) that can be used in order to predict forward ($t + \Delta t$). Thus it measures the length of the "memory" of the time series.

The coefficients γ_j and the parameter P_{M+1} are determined as presented by Burg (1967, 1968) and

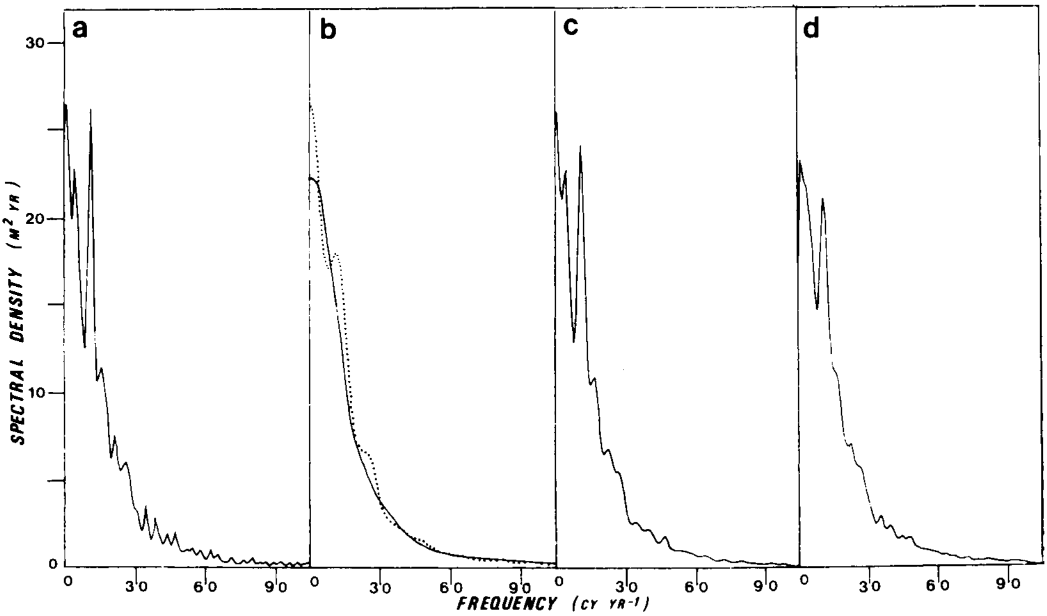

Fig. 1. Five versions of the spectrum of the 8th component. The values of parameter M are (a) 245, (b) 35 (full line) and 64 (dotted line), (c) 120. Case (c) seems to be closest to the classical spectrum computed with the Parzen window (d). Computed from the time series of the years 1962–70.

Table 1. The filter lengths of some EOFs in different samples; the EOF index is ν.

	Sample			
ν	1946–55	1955–62	1962–70	1966–79
1	50	44	64	77
2	11	30	16	22
3	12	25	44	41
4	28	44	46	61
8	4	43	64	73
9	10	46	36	54
10	3	20	17	27
12	2	18	57	65
20	8	50	61	62
28	3	21	40	75
40	6	16	22	48
65–170	7–1	5–2	9–1	34–2

used in, for instance, Smylie et al. (1973). The filter length is determined from the Akaike criterion (1969a, b), which is called the final prediction error criterion (FPE):

$$(\mathrm{FPE})_M = \frac{L + M + 1}{L - M - 1} P_M, \qquad (2)$$

where L is the number of observations and M is the filter length. The larger M is, the more details there are in the spectra (cf. Figs. 1a–1c). The optimum value of M is the one minimizing the FPE. The degrees of freedom in the resulting spectra (Fig. 1b, $M = 64$) are clearly higher than in the classical spectra (Fig. 1d compares with Fig. 1c, where $M = 120$, cf. Appendix). Problems of the MEM are presented in more detail in the Appendix.

The spectra of the coefficient series have been computed for samples 1946–55, 1955–62, 1962–70 and 1966–79. The components $\nu = 1, 2, \ldots, 29, 30, 35, 40, \ldots, 170$ have been studied. Values of the parameter M are listed for some components in Table 1. Differences between adjacent components are due partly to analysis errors and partly to physical differences. The memory length increases when data become better. The memory length tends to become shorter with increasing component number, except for the short filters of some components like $\nu = 2$ and $\nu = 10$. Von Storch and Fischer (1983) used a value of M which is $\frac{1}{3}$ of the length of the time series. In our case, the filter length is a function of the EOF index. The M values clearly show that the time series of EOF components differ in character.

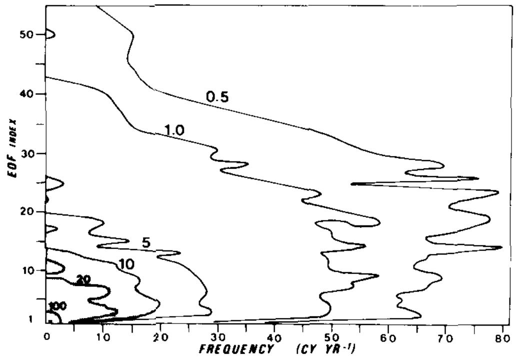

Fig. 2. The spectral density of the 500 mb geopotential height (m^2 year) as a function of EOF index and frequency. There is no pre-whitening, i.e., the yearly oscillation is included. The point in the lower left corner corresponds to over 10,000 m^2 year. Computed from the time series of the years 1962–70.

The spectral density is highest at small index components and for long periods (Fig. 2). The density distribution has the form of red noise on which smaller deviations (peaks) are superimposed. An exception is the first component which has its main variance in the yearly oscillation. The other samples show a similar structure.

4. The peaks

The spectral peaks are determined from all four samples. The significance of the peaks can be studied by comparing the results of different samples. Most of the spectra of the sample 1946–55 are too smooth, so that normally only three samples can be compared.

The location and intensity of the peaks are determined by subtracting the background spectrum from the main spectrum. Thus the assumption of the structure of the background spectrum may have an effect on the results. That assumption is discussed in Rinne and Sarkanen (1983a), where a general red form for the background spectra is derived. An example is shown in Fig. 3. Because the background spectrum is an estimate, some values in Fig. 3 are slightly negative. This does not prevent the identification of peaks (cf. Appendix).

In the case of the low-indexed components (up to about $\nu = 50$), indications of distinct peaks were observed. The high-indexed components usually

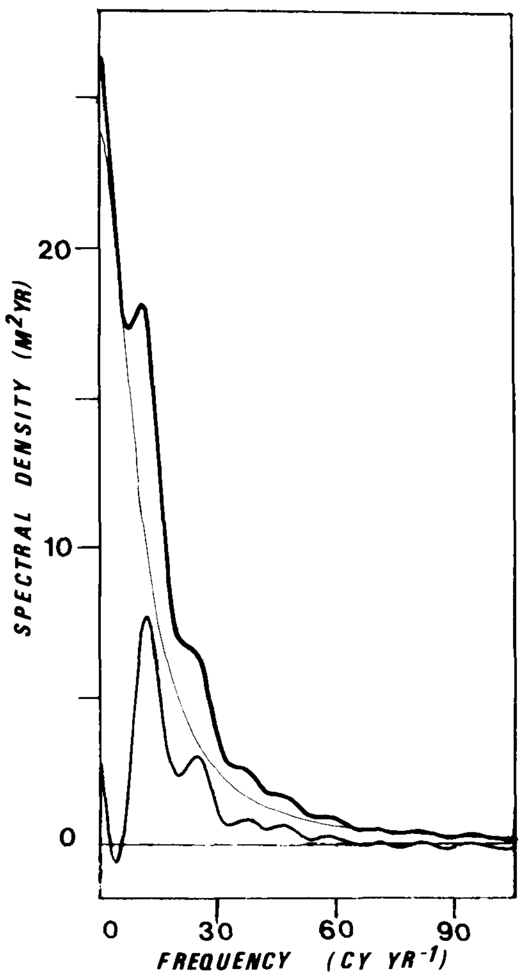

Fig. 3. The original spectrum (thick upper line), background spectrum (thin line) and their difference (thick lower line) of the 8th function. Computed from the time series of the years 1962–70.

have only one or two broad peaks. The peaks are listed in Tables 2–5. In most cases the peaks are required to be present in all three samples (exceptions are the peaks at about $f = 40$ cpy (cycles per year) and $f = 14$ cpy). The main peaks are indicated with an asterisk. The types of spectra observed have been grouped as follows:

0. The first component.
1. One single well-identified peak in the spectrum.
2. A number of peaks, the main peak being at $f \sim 12$ cpy.
3. A number of peaks, the main peak(s) being at $f \sim 20$ cpy.

Table 2. *Peak frequencies of the components with a single peak*

	Sample			
ν	1945–55	1955–62	1962–70	1966–70
2	23	22	24	21
3	20	21	22	16
10	—	23	22	22
4	—	21	15	18

Unit: cycles per year: ν is the EOF index.

Table 3. *Peak frequencies of components with the main peak at 12 cpy*

ν	Sample	Peaks (cpy)								
5	1955–62	11*		30		50				
	1962–70	15*		32			58			
	1966–79	14*		29		45	60			
6	1955–62	8*	21					67		
	1962–70	9*	24		41			74		
	1966–79	10*	21					75		
7	1955–62		19					66		
	1962–70	9*	24		41			74		
	1966–79	10*	20					68		
8	1955–62	12*				47	63		80	
	1962–70	11*	23		37	48	61		82	
	1966–79	12*	20		39	49	60		83	
9	1955–62	12*	25		38			71		89
	1962–70	13*						72		98
	1966–79	14*	20		41			69		93
11	1955–62		47					71		
	1962–70	10*	19		43		57	72		
	1966–79	8*	17		41		57	73		
12	1955–62	14*	25*		39		60	75		90
	1962–70	14*	28*		41		61	74		89
	1966–79	14*	24		37		60	75		90

Given frequencies are as observed in three samples. The main peaks are indicated with an asterisk and ν is the EOF index

4. A number of peaks, the main peak(s) being at larger frequencies.

The grouping is done subjectively and the purpose of grouping is to make it easier to compare different spectra. The grouping seems to reflect the order of the functions (Tables 2–5). The following limitations must be taken into account. The low-frequency peaks ($f < 6$ cpy) are obviously outside the present study (cf. discussion of the filter length

Table 4. *As Table 3, but for components with the main peak at 20 cpy*

ν	Sample	Peaks (cpy)							
13	1955–62		23*		40		57	73	
	1962–70		22*		40		56	78	
	1966–79		17*		40		56	74	
14	1955–62		22*			46		80	
	1962–70		21*	33*		52		74	
	1966–79	15	25*			59		75	
15	1955–62		18*	32			64		85
	1962–70	14*		29*	45		62		81
	1966–79	15		26*	38		62		87
16	1955–62		17*		40			77	
	1962–70		21*		44			68	
	1966–79	12	21*		36			73	
17	1955–62		21*		41		61		
	1962–70		21*		42		64		
	1966–79	15		29*	45				
18	1955–62	—							
	1962–70	6		25*	39	56		70	84
	1966–79	11*	21*		40*	53		70	83

M in the Appendix). Peaks at $f > 80$ cpy are only partly listed. As previously discussed, the intensity and locations of peaks depend somewhat on *M* and on the red background spectrum. The application of the FPE criterion results in quite smooth spectra. Separation of adjacent peaks is then impossible.

In some cases, the spatial patterns of the EOFs are characterized in terms of zonal wavenumbers in order to show the scale of the functions, though the EOFs may differ from wavy patterns. Fig. 4c shows an extreme case where the pattern consists of one local cell. In Fig. 4d the pattern forms a meridional wave train. The patterns in Figs. 4a, b can be quite easily characterized with zonal wavenumbers.

Group 0. The total variance of the first component is about 14,000 m^2 in all samples (57% of the total variance). The annual and semi-annual terms explain 98.5% and 0.5%, respectively. The remaining part shows no distinct peaks. The other components explain less than 4% of the yearly cycle.

Group 1. Components with a single broad peak. The components and peak frequencies are listed in Table 2. The peaks of the components $\nu = 2$ and 10 are very persistent through all subsamples (cf. Fig. 5). Note that the peak at 3 cpy in Fig. 5 is due to the way of presentation ($fS(f)$), which generates a high-pass filtering. Therefore it is not a true one.

Table 5. *As Table 3, but illustrating components with a main peak at 30–60 cpy* (ν = *20, 24, 25*), *with a number of similar peaks at 10–80 cpy* (ν = *28*) *and some high-indexed components with obvious peaks* (ν = *45, 100*).

ν	Sample	Peaks (cpy)									
20	1955–62	11		29*		44					
	1962–70	11		26		47*	59	73	86	105	119
	1966–79	12		27		47*	60	73	86	107	120
24	1955–62		14	31			60	73			124
	1962–70		17*	36*				75			121
	1966–79	12		34*			60	74			121
25	1955–62	11		31*		47	62				
	1962–70	11*		32*		44	58		84		
	1966–79	11*		32*			56		85		
28	1955–62	12		29		46*	65		84	110	
	1962–70		15*		33				79	100	119
	1966–79	4	15*	24*	34*		61*		82*	101	121
45	1955–62				34		63			125	
	1962–70				35		63			123	171
	1966–79				41		68			111	150
100	1955–62										165
	1962–70										140
	1966–79							115			180

In comparison with those in the other spectra, the peaks are very broad. If the width of the peak is defined by one-half points, then for example in the case of the 2nd component, the width is about 18–30 cpy in every sample.

In addition to those listed, the 3rd component has a peak at 12 cpy in sample 1962–70. Similarly the 4th component has a peak at 7 cpy in 1955–62. The patterns of components 2 (Fig. 4a), 3 and 10 show features of ultralong waves. Their main zonal wavenumber is 1–2. The main zonal wavenumber of the 4th pattern is 3.

Group 2. Components with the main peak at 12 cpy usually have a number of additional peaks, as is seen in Table 3. There is another permanent but weaker peak at 20 cpy. A 5-day peak (72 cpy) is found in nearly every sample and component. However, its spectral power is weak in a single spectrum.

Note that for illustration purposes, all peaks at $f \sim 40$ cpy are listed, though some of them are present only in a single sample. In Fig. 6, the spectrum of the 12th component is shown. It is possible that the peak at $f = 28$ cpy, in sample 1962–70, is split into two parts (cf. Appendix), at $f = 24$ cpy and $f = 37$ cpy, in sample 1966–79. The latter part was then folded on a "true" peak at $f = 40$ cpy. In Table 3 (and in other similar cases) the peaks are given as such.

The functions $\nu = 6$, 8 (Fig. 4c), 9 and 12 represent single, vast local cells, whereas the functions $\nu = 5$, 7 and 11 have wavy patterns. The wavelengths correspond to wavenumbers of about 3–4.

Group 3. The main peak is at 20 cpy (Table 4). The functions of this group are not easy to characterize with wavenumbers except function $\nu = 14$, which shows quite a regular wave with the zonal wavenumber 5 (Fig. 4b). Some of the peaks at 20 cpy (e.g. $\nu = 15$) seem to be replaced by two separate peaks in 1966–79. This may be an indication of an unsuitable value of M in some samples.

Group 4. Only some components of this group are shown in Table 5. In contrast to Fig. 7, Fig. 8 shows a case of more poorly coinciding peaks at lower frequencies. There are indications of peak splitting. The single peak at $f = 29$ cpy in sample 1955–62 may be represented by two (1962–70) or three (1966–79) separate peaks in other samples. The high frequency peaks coincide rather well in Fig. 8 as in Fig. 7.

In components $\nu > 30$, the intensity of longer periods becomes weaker. High-indexed compo-

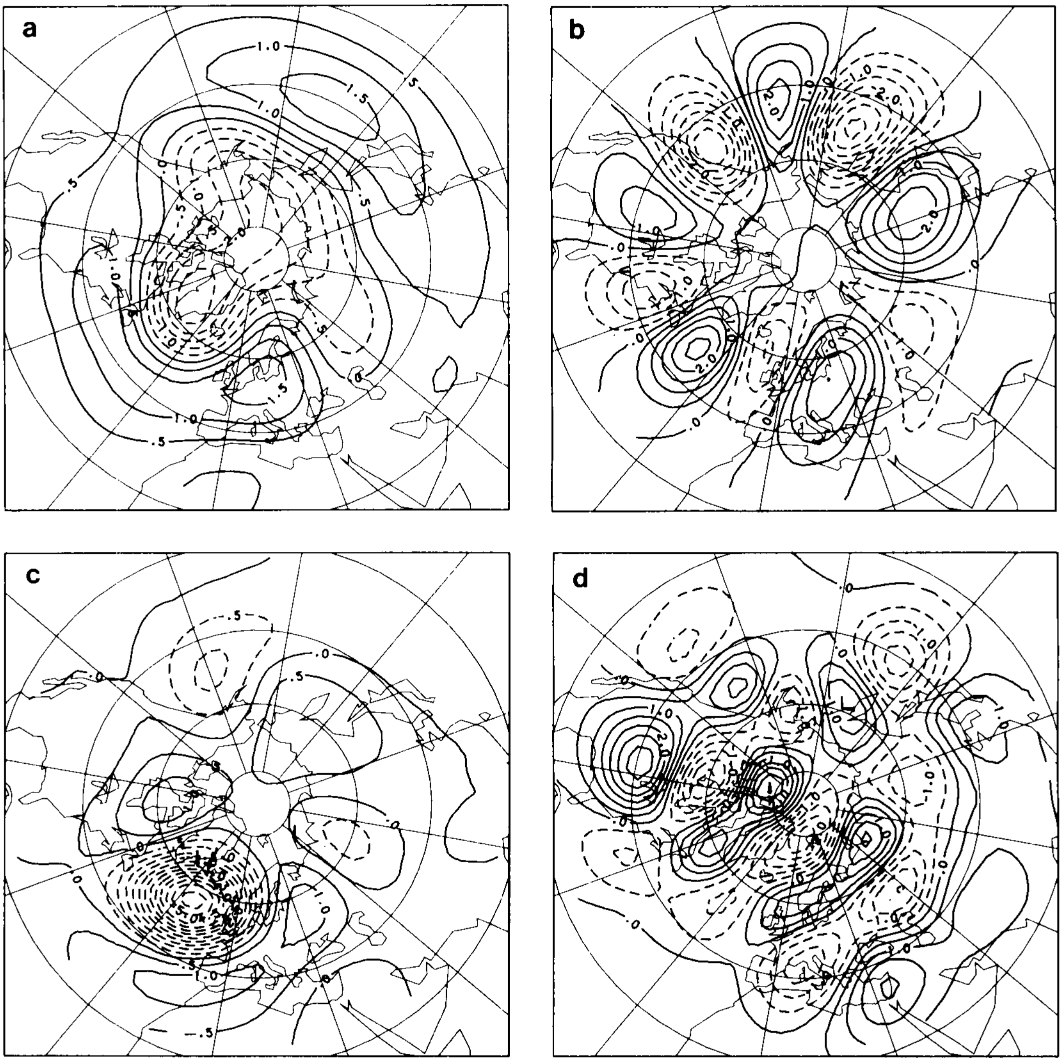

Fig. 4. EOF patterns for components ν = (a) 2, (b) 14, (c) 8, (d) 32. The spacing of the isolines is 0.5. Full lines indicate positive and broken lines negative values, respectively.

nents often have only weak high-frequency peaks, which do not persist from sample to sample. Thus, these spectra can be considered mainly as being those of red noise. However, note that the filter length applied was short (cf. Fig. 10b).

5. Discussion

It is obvious that some significant peaks have been found. For instance the peak at $f \sim 12$ cpy is present in so many spectra of different components that it could well be a real one. On the other hand it is impossible to tell immediately the phenomenon or phenomena behind the cycles.

One of the peaks has been studied in detail (Rinne and Sarkanen, 1983b): that at 22 cpy in the spectrum of the 2nd component. The cycle was separated from the time series of the component by applying a suitable band-pass filter. The resulting time series shows an oscillation which is cyclic with a period of roughly 16 days. After the dates of the maxima were determined, the corresponding 500 mb analyses were picked out and the composite

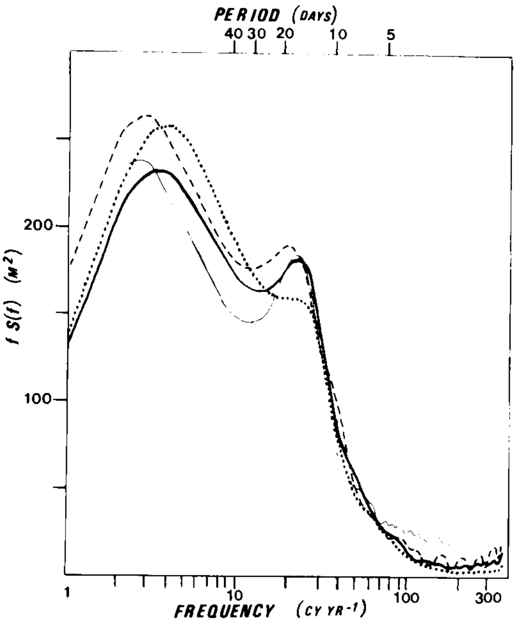

Fig. 5. The spectrum (frequency times the spectral density) of the 2nd component in sample 1946–55 (thin full line), 1955–62 (broken line), 1962–70 (dotted line), 1966–79 (thick full line).

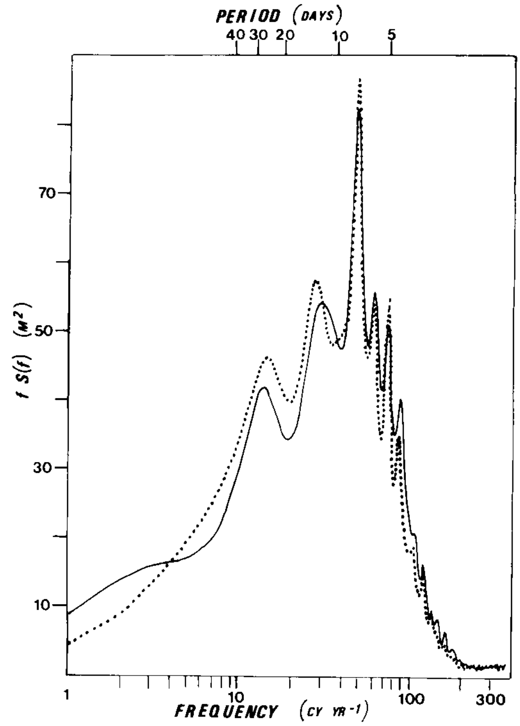

Fig. 7. The spectrum of the 20th component in sample 1962–70 (dotted line) and 1966–79 (thick full line).

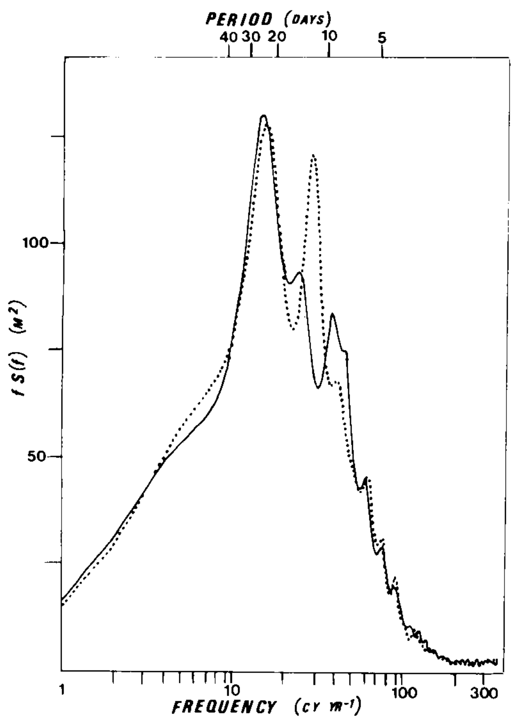

Fig. 6. The spectrum of the 12th component in sample 1962–70 (dotted line) and 1966–79 (thick full line).

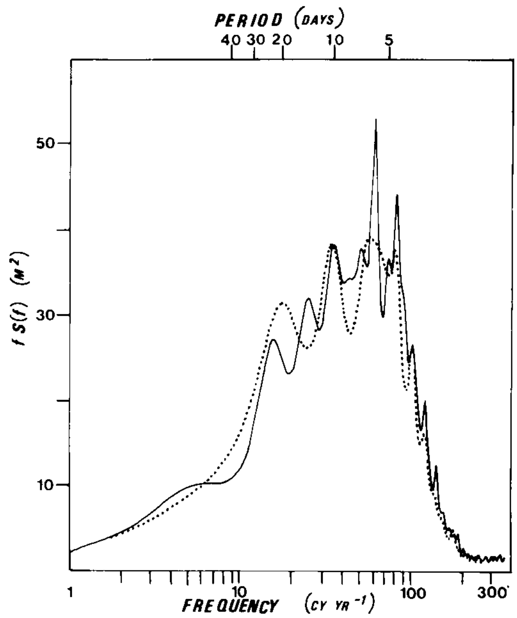

Fig. 8. The spectrum of the 28th component in sample 1962–70 (dotted line) and 1966–79 (thick full line).

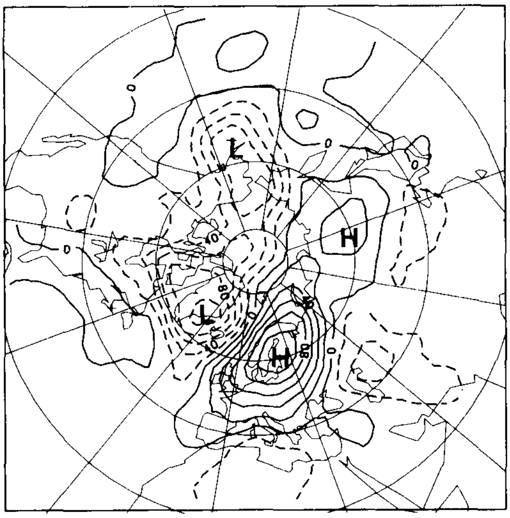

Fig. 9. Composite map with key dates at the maxima of the 16-day wave in the 2nd EOF. Computed as a mean anomaly of the 500 mb height analyses during winters 1962–70. The spacing of the isolines is 20 gpm. Full lines indicate positive and broken lines negative values, respectively.

maps were computed. One of such maps is displayed in Fig. 9. It shows a hemispheric wave with lows and highs on the western and eastern part of the northern hemisphere, respectively. It turns out that the wave is not strictly connected to the 2nd EOF. The pattern in Fig. 9 differs from that in Fig. 4a. In other phases of the wave, the difference is larger. The 16-day wave is only a weak signal in the time series of the 2nd component. Thus the structure of the wave could not be predicted from the pattern of the 2nd EOF. This EOF has only been an indicator by which the phenomenon has been traced. The minimum map (corresponding to minimum days of the time series) turns out to be nearly a mirror image of Fig. 9 with highs and lows interchanged. The composite map of other phases indicates that the wave mainly moves westward. All these observations and the structure of the wave show that the wave can be associated with the classical 16-day wave.

From the case study presented, it is seen that each of the peaks must be studied separately. Obviously it is fruitless to study more deeply the significance of the peaks or properties of single EOF's. Instead, it is important to determine correctly the key dates of the phenomenon from a large enough sample.

In group 2 (Table 3), one or more cycles are visible at $f = 12$ cpy (8–14 cpy). Applying Salby's (1981b) results, individual normal modes at such a long cycle (cycles) would not be identifiable. In terms of the dimensionless frequency used by Salby, the frequency of the cycle is 0.015. Because the "temporal uncertainty under typical conditions" is 0.013, 0.025 and 0.038 for the zonal wave numbers $m = 1, 2, 3$ respectively, such a cycle should be at or beyond the limit of identification. On the other hand applying Salby's Fig. 4, peaks at $f = 22, 40, 50, 72, 80–90$ cpy (or in days, ca 16, 9, 7, 5, 4.5–4) can correspond to modes $(m, n - m) = (1, 3), (1, 2), (2, 2), (1, 1), (2–3, 1)$, for instance. All of those should be identifiable. The cycles at $f = 60$ cpy and $f = 30$ cpy cannot clearly be identified from Salby's Fig. 4.

In other groups the discussion is similar. One finds candidates for different identifiable modes. The cases of $f = 12$, 30 and 60 cpy can similarly be found. New peaks are picked from the right-hand end of the spectra. The peak at $f \sim 150$ cpy ($\nu = 45,100$) could correspond to Rossby-gravity modes with $n - m = 0$. The peak at $f \sim 120$ cpy ($\nu = 20, 24, 28, 45$) is not present in modes discussed by Salby (1981b).

6. Concluding remarks

Because no seasonal correction has been applied to the time series, the results correspond best to the seasons with the most intense variation in the actual frequency range, i.e., the results most often represent conditions in the winter half of the year.

A number of spectral peaks of the 500 mb geopotential height can be found with the aid of EOFs. Long-period peaks tend to appear as dominating ones in the spectra of small-indexed components in the range of 1–5 weeks. The medium-indexed components tend to have more peaks at shorter periods of equal importance. The peaks of the high-indexed components are weak and difficult to identify.

It is obvious that many of the peaks are real. One of them has been associated with the 16-day wave applying the composite map technique. Before a similar study of wave structure is done for the other peaks, they can only be tentatively associated with the normal mode frequencies. We have found peaks at the frequencies of the symmetric Rossby modes

(16, 5, 4.5–4 days), antisymmetric modes (9, 7 days) and the Rossby-gravity modes (2.5 days). The cycles at 12, 6 and 3 days cannot clearly be connected with any Rossby modes. Periods of about 5 weeks are clearly present in many components, though such periods should be at the limit of identification according to the theoretical studies of the normal modes. No group of candidates for a 24-day vacillation was found.

The connections to (and differences from) the Rossby modes are only tentative ones. Final conclusions require detailed studies of the time series. Some interesting questions arise such as do the 16-day peaks correspond to the 16-day wave as is the case in the 2nd component; what are the distinct peaks at periods of 5 weeks; what are the 3, 6 and 12 day peaks, how many of the 5-day peaks correspond to the 5-day wave, can the 9- and 7-day peaks really be associated with antisymmetric modes?

7. Acknowledgements

This work has been financially supported by the Academy of Finland.

8. Appendix. Properties with applying the maximum entropy method

8.1. Problems

It is difficult to uniquely determine the optimum value of M. A short filter gives a smooth spectrum without details and a longer filter generates spurious peaks (Fig. 1a, b). In Fig. 10a, there are three different possibilities when the FPE-method is used: $M = 64$, $M = 75$ or $M = 92$. Each of them reaches the level of the absolute minimum. In the present paper, we follow the principle of the "first absolute minimum". Thus we take $M = 64$, i.e., the filter is 32 days long ($\Delta t = 0.5$ days). However, in cases like Fig. 10b, a stronger constraint is applied (from Fig. 10b we take $M = 3$).

The principle of "the first absolute minimum" causes almost no peaks to be found in time series of the years 1946–55. Thus, the principle is rather too strong than too weak, which is in agreement with von Storch and Fischer (1983). They argue that the FPE criterion tends to underestimate the value of M, i.e., the spectra tend to become too smooth. Of course, other reasons for the lack of peaks are the resolution ($\Delta t = 1$ day) and the large analysis error for that period.

It is possible that the MEM cannot find long-period peaks, when the length of the period is much longer than M. For instance, Fourier analysis indicates that the 2nd component has a weak half-yearly oscillation. It was not found by MEM. This is connected with the length of the filter, which for $\nu = 2$ is only 20, corresponding to a "memory" length of 10 days. When the filter length is increased up to $M = 150$, the half-yearly peak is found. On the other hand, the very strong yearly oscillation of the first component was easily detected, though the filter was quite short, $M = 64$.

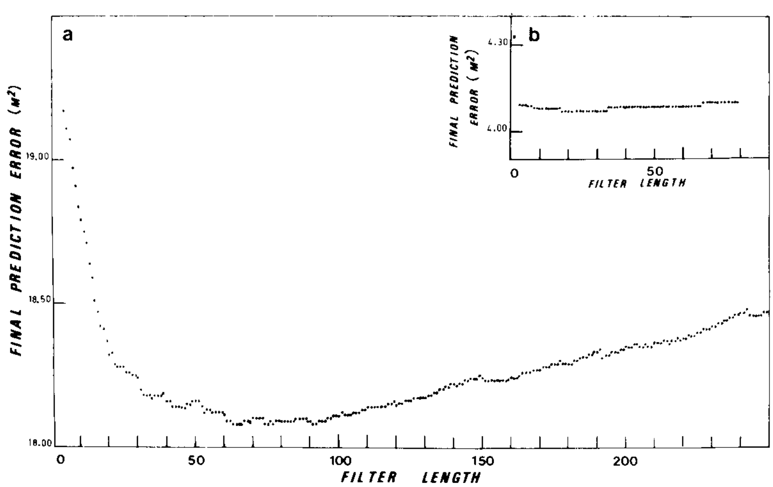

Fig. 10. The final prediction error, FPE, (m^2) of (a) the 8th component and (b) the 100th component as a function of the filter length M. Computed from time series of the years 1962–70.

Here the problem is solved by studying periods shorter than 5 weeks.

Thus far, there exist no significance tests for the MEM (Hayashi, 1981). The longer the filter length the more details are shown in the spectrum. The more details appear, the less significant they probably are. The only test method seems to be to make use of subsamples which are then compared with each other.

8.2. Experiences

Because we have had the possibility of comparing different samples, some observations concerning M and the FPE-criterion could be made.

In the case of component 15, sample 1962–70, the spectrum was computed with $M = 37$, 40 and 46. Values of 40 and 46 correspond to the absolute and a local minimum of the FPE-criterion, whereas 37 is an arbitrary value, which does not fulfil the FPE-criterion. The peaks of the spectra of $M = 40$ and 46 are similar, whereas those of $M = 37$ differ. Because such a small downward deviation from the criterion caused large changes when M is quite small, only exceptionally do we deviate from the criterion. The classical spectral method results similarly in different spectra, when the maximum lag is suitably changed from a larger value to a smaller one.

It was previously stated that the M values of the sample 1946–55 are too small when compared to the other samples. In addition to that, M values of sample 1955–62 are often smaller than those of the following samples. Consequently, the spectra are smoothed. Therefore when studying peaks, we sometimes applied a larger value of M, making use of a local FPE minimum. Such values produced peaks similar to the ones of the other samples. However, a larger M is only applied in a few spectra.

Ulrych and Bishop (1975) present a case, where a peak was split into two adjacent ones when M was increased. We have seen the same phenomenon in some spectra. For instance, the strict application of the principle of the "first absolute minimum" gives $M = 44$ for component 3 in sample 1962–70. The corresponding spectrum differs from those of the other samples because the peaks are split, whether correctly or not. Another choice is to use a much smaller value of $M = 23$, which represents a local minimum of the FPE criterion. Applying that value, makes the spectrum of the sample 1962–70 similar to those of the other samples. A candidate for peak splitting is illustrated in Fig. 6. Such cases are discussed in Section 4 of the main test.

Sometimes the spectrum is not sensitive to changes of M. The peak of component 2 (sample 1962–70) is well produced even if M is increased from $M = 16$ up to $M = 500$. Some spectra show no strong peaks. This property may remain even though M is much increased. Normally such an increase of M generates new peaks. We have drawn the conclusion that insensitivity to changes in M indicates more reliable results. However, this conclusion has not been applied to the present paper.

The application of the MEM may seem to be arbitrary because different values of M give different spectra (Figs. 1a, b). However, this is a typical feature of spectrum analysis: the more details there are, the less reliable they are. In the classical analysis, a small maximum lag and a suitable smoothing window give a smooth spectrum. In our case, a maximum lag of 365 time increments (half a year) and the Parzen window could be suitable. Such a spectrum is shown in Fig. 1d. It turns out that this spectrum is close to the MEM spectrum with $M = 120$ (Fig. 1c). This seems to be valid for all other EOFs; usually $M = 120$ gives spectra resembling the classical ones.

In the classical analysis, "a constant M" is taken when choosing the maximum lag and the window. Usually the main interest is in the statistical significance of the peaks. In the present case, the choice of M depends on the quality of the time series. The more noise there is and the shorter the length of the memory, the less detailed is the spectrum. The main interest is in the persistency of the peaks. Because M is always less than 120 (Table 1), it is obvious that the degreees of freedom of the present spectra are much greater than in the classical spectra such as the one in Fig. 1d.

The peaks in the classical spectrum of Fig. 1d are not significant. If the peaks of the MEM spectrum in Fig. 1c could be tested similarly, then the peak at $f = 12$ cpy would be significant.

8.3. Summary

We have sometimes deviated from the principle of the first absolute minimum. In a few cases, it seemed to be reasonable to apply M values given by a local minimum. Such modifications must be carried out with caution, because small changes in

M may change the spectrum. If the form of the spectrum is independent of M, then the spectrum is believed to be more reliable. In the present spectra, the degrees of freedom are clearly greater than in the corresponding conventional spectra.

The background spectra

The background spectra have been determined from

$$S_v(f) = A_v/(f^2 + \lambda_v^2), \quad (A.1)$$

where f is frequency. Parameters A_v and λ_v are computed from

$$\lambda_v = av^b$$
$$A_v = c20^{-d}, \quad 1 < v \leqslant 20, \qquad (A.2)$$
$$cv^{-d}, \quad 20 < v.$$

The values of constants a, b, c and d have been determined empirically in Rinne and Sarkanen (1983a). For instance, in the case of the analyses 1962–70 we have $a = 2.0$, $b = 0.81$, $c = 100{,}000$ and $d = 1.25$. Note, that these parameter values fully determine the background spectra of all components in the whole frequency range utilized.

REFERENCES

Akaike, H. 1969a. Fitting autoregressive models for prediction. *Ann. Inst. Stat. Math. 21*, 243–247.

Akaike, H. 1969b. Power spectrum estimation through autoregressive model fitting. *Ann. Inst. Stat. Math. 21*, 407–419.

Blackmon, M. L. 1976. A climatological spectral study of the 500 mb geopotential height of the northern hemisphere. *J. Atmos. Sci. 33*, 1607–1623.

Bradley, J. H. S. and Wiin-Nielsen, A. 1968. On the transient part of the atmospheric planetary waves. *Tellus 20*, 533–544.

Burg, J. P. 1967. Maximum entropy spectral analysis. Paper presented at *the 37th Annual International Meeting Soc. of Explor. Geophysics*. Oklahoma city, Okla., Oct. 31.

Burg, J. P. 1968. A new analysis technique for time series data. Paper presented at *Advanced Study Institute on Signal Processing*, NATO, Enschede, Netherlands.

Deland, R. J. 1965. Some observations of the behavior of spherical harmonic waves. *Mon. Wea. Rev. 93*, 307–312.

Dikii, L. and Golitsyn, G. 1968. Calculation of the Rossby wave velocities of the earth's atmosphere. *Tellus 20*, 314–317.

Eliasen, E. and Machenhauer, B. 1969. On the observed atmospheric wave motions. *Tellus 21*, 149–165.

Fräedrich, K. and Böttger, H. 1978. A wavenumber-frequency analysis of the 500 mb geopotential at 50° N. *J. Atmos. Sci. 35*, 745–750.

Hayashi, Y. 1981. Space-time cross spectral analysis using maximum entropy method. *J. Meteorol. Soc. Japan 59*, 620–624.

Kasahara, A. 1980. Effect of zonal flows on the free oscillations of a barotropic atmosphere. *J. Atmos. Sci. 37*, 917–929.

Madden, R. A. and Julian, P. 1972. Further evidence of global-scale 5-day pressure waves. *J. Atmos. Sci. 29*, 1464–1469.

Madden, R. A. 1978. Further evidence of traveling planetary waves. *J. Atmos. Sci. 35*, 1605–1618.

Madden, R. A. 1979. Observations of large-scale traveling Rossby waves. *Rev. Geophys. Space Phys. 17*, 1935–1949.

McGuirk, J. P. and Reiter, E. R. 1976. A vacillation in atmospheric energy parameters. *J. Atmos. Sci. 33*, 2079–2093.

Peacock, K. L. and Treitel, S. 1969. Predictive deconvolution: theory and practice. *Geophysics 34*, 155–169.

Rinne, J. and Järvenoja, S. 1979. Truncation of the EOF series representing 500 mb heights. *Q. J. R. Meteorol. Soc. 105*, 885–897.

Rinne, J. and Karhila, V. 1979. Empirical orthogonal functions of 500 mb height in the northern hemisphere determined from a large data sample. *Q. J. R. Meteorol. Soc. 105*, 873–884.

Rinne, J., Karhila, V. and Järvenoja, S. 1981. The EOF's of the 500 mb height in the extratropics of the northern hemisphere. *Report* no. 17, *Dept. of Meteorology, University of Helsinki*, Finland, 16 pp + Appendix.

Rinne, J. and Sarkanen, A. 1983a. The 500 mb geopotential height as a first-order Markov process. *Proceedings II International Meeting on Statistical Climatology*. Lisboa, Portugal, 26–30 September 1983, 16.3.1–16.3.6.

Rinne, J. and Sarkanen, A. 1983b. The 16-day peak in the second EOF of the 500 mb geopotential height. *Proceedings II International Meeting on Statistical Climatology*. Lisboa, Portugal, 26–30 September 1983, 11.8.1–11.8.6.

Salby, M. L. 1981a. Rossby mormal modes in nonuniform background configurations. Part I: Simple fields. *J. Atmos. Sci. 38*, 1803–1826.

Salby, M. L. 1981b. Rossby normal modes in nonuniform background configurations. Part II: Equinox and solstice conditions. *J. Atmos. Sci. 38*, 1827–1840.

Schäfer, J. 1979. A space-time analysis of tropospheric planetary waves in the northern hemisphere. *J. Atmos. Sci. 36*, 1117–1123.

Smylie, D. E., Clarke, G. and Ulrych, T. J. 1973.

Analysis of irregularities in the earth's rotation. *Methods in computational physics*, *13*, 391–430, Academic Press, N.Y.

Ulrych, T. J. and Bishop, T. N. 1975. Maximum entropy spectral analysis and autoregressive decomposition. *Rev. Geophys. Space Phys. 13*, 183–200.

Webster, P. J. and Keller, J. L. 1975. Atmospheric variations: Vacillations and index cycles. *J. Atmos. Sci. 32*, 1283–1300.

Willson, M. A. G. 1975. A wavenumber-frequency analysis of large-scale tropospheric motions in the extratropical northern hemisphere. *J. Atmos. Sci. 32*, 478–488.

Von Storch, H. and Fischer, I. 1983. An analysis of geopotential height at 300 mb in the frequency wavenumber domain along 50° N is observed and modelled January climate. *Beitr. Phys. Atmos. 56*, 199–212.